Polymer Bulletin
https://doi.org/10.1007/s00289-023-05037-4

ORIGINAL PAPER

Preparation of organic–inorganic bio-based epoxy coatings with high anti-corrosive performance

Semiha Eral[1,2] · Burcu Oktay[2] · Cemil Dizman[1] · Nilhan Kayaman Apohan[2]

Received: 29 March 2023 / Revised: 12 September 2023 / Accepted: 17 October 2023

Abstract

Epoxies derived from natural sources as an alternative to conventional petroleum-based epoxy resins have been used in sustainable coating applications. This study aims to create corrosion-resistant bio-based epoxy nanocoatings in the context of sustainable development. For this purpose, vegetable oil-based epoxy resins from cardanol and soybean oil were prepared. The structure of bio-based epoxies was confirmed by FTIR and ^{1}H-NMR spectroscopy techniques. The epoxy functional silane precursor is synthesized from tetraethyl orthosilicate and (3-Glycidyloxypropyltrimethoxysilane by means of the sol–gel method. Amine curing agent and inorganic silica skeletons as polyhedral oligomeric silsesquioxanes and sol–gel precursor were added to the epoxy adduct and then cured. The curing kinetics of the formulations was followed by a differential scanning calorimeter. The chemical, mechanical, thermal, and anti-corrosive properties of the prepared coatings were investigated using various tests. The sustainable epoxy-based nanocoatings exhibited higher mechanical and thermal stability. In addition, the nanocoatings showed excellent corrosion resistance without the use of any anti-corrosive agent. The prepared green sustainable coatings will provide a more sustainable way to prepare bio-based coatings.

Graphical abstract

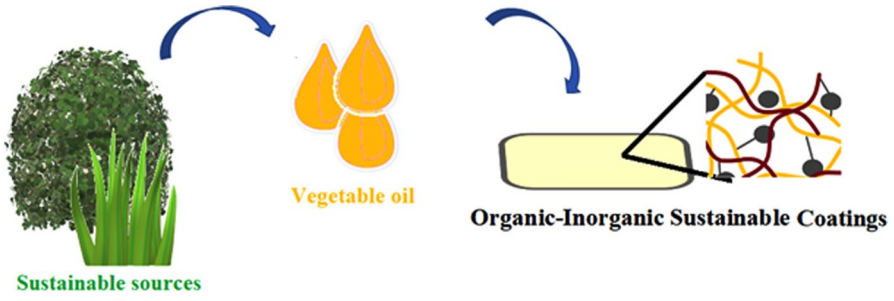

Extended author information available on the last page of the article

Published online: 31 October 2023

Keywords Anti-corrosive coating · Organic–inorganic coating · Sustainable resources · Vegetable oil

Introduction

In recent years, the utilization of renewable resources in the coating industry has attracted the world's attention as a green alternative to fossil resources due to environmental issues and the problem of the non-renewability of fossil resources [1]. Vegetable oils (VOs) such as castor oil, linseed oil, hempseed oil, and soybean oil have become popular in renewable resources, which have been used for the development of polymeric systems by a variety of polymerization processes [2]. The chemical structure of vegetable oils contains three fatty acid sections and the active different functional groups such as hydroxyl groups, ester groups, and double bonds. The presence of these groups allows for further modification of the vegetable oils [3].

Cardanol can be used important starting material in the polymer industry due to its widespread availability and low cost [4]. It has multiple functional groups the aromatic ring, phenolic hydroxyl group, and unsaturated side chain. The presence of an aromatic ring on the main backbone provides the enhancement of thermal stability. In addition, the long alkyl chain of cardanol increases hydrophobicity [4, 5]. Cardanol derivatives can be prepared by etherification, esterification, sulfonation, and epoxidation [6].

Diglycidyl ether of bisphenol A (DGEBA) is currently the monomer most frequently employed in the manufacture of epoxy polymers and materials. However, DGEBA has adverse effects on human health and the environment [7]. Epoxy-cardanol is a new and sustainable friendly alternative to DGEBA. The epoxy-cardanol can be synthesized by two pathways. In the first method [8], the phenolic hydroxyl group of cardanol reacts with epichlorohydrin in the presence of $ZnCl_2$. In the second method [9], the double bonds of cardanol alkyl side chains are epoxidized by H_2O_2 in the presence of an acid catalyst.

Epoxide network is a class of thermoset materials, obtained by curing epoxy resins with various diamines at different temperatures. The usage of epoxide networks in coatings and adhesives is widespread [10]. However, epoxy resin made from vegetable oils also suffers from brittleness issues [11]. In recent years, porous materials based on polyhedral oligomeric silsesquioxanes (POSS) have attracted a lot of commercial interest [12]. By adding POSS to the polymer matrix, high-performance materials were obtained with strong thermal and mechanical strength properties [13]. Zahn et al. investigated the fire resistance of diglycidyl ether of bisphenol A-based epoxy resin by adding silsesquioxanes. The results indicated that the char of the nanocomposite materials strongly increased with the involvement of Si–O bonds [14]. Yonggang et al. showed that silsesquioxanes significantly improved gallic acid-based epoxy resin of mechanical properties, dynamic mechanical properties, and thermal stability [11]. Florea et al. developed novel epoxy bisphenol A resin reinforced with POSS based on nanocomposites. The nanocomposite exhibited the highest storage modulus and hardness due to the cages effect of POSS [15].

To overcome the brittleness of bio-based composites also, silane coupling agents can be used. Moreover, the introduction of silane coupling agents provides coatings with additional functionalities such as corrosion resistance, and water resistance, [16]. In recent years, silane coupling agents have become high-performance additives. The functional groups can attach to the cave structure of POSS. Vinyl, epoxy, or NH_2-modified POSS improves the both physical and chemical performance of the polymer by increasing the interfacial interaction between the polymer matrix and POSS [17].

The purpose of this study is to create organic–inorganic hybrid bio-based coatings based on vegetable oils and inorganic silica skeleton (silsesquioxanes and sol–gel). The epoxy-functional silane sol–gel precursor and vinyl POSS reacted with each other via silanol groups. In addition, the epoxy functional groups of the sol–gel precursor and epoxy resins created the crosslinked network by epoxy-amine bonding. The organic–inorganic hybrid structures were achieved straightforwardly and feasibly. The Si–O inorganic network resulted in the improvement of the thermal and mechanical properties of the bio-based coatings.

Materials and methods

Materials

Soybean oil (Sam Yagcilik Pazarlama A.S.), cardanol (Cardolite Specialty Chemicals) and diglycidyl ether bisphenol A (DGEBA) resin (EPON 828, Hexion) were used without purification. Tetraethyl orthosilicate (TEOS, 98%), (3-glycidyloxypropyl)trimethoxysilane (GPTMS, $\geq$ 98%), (3-Glycidyl)propoxy-heptaisobutyl substituted (EPOSS), hydrogen peroxide (33%), sulfuric acid (98%), epichlorohydrin, zinc chloride, sodium hydroxide, and triethylenetetramine (TETA) were used as purchased from Sigma-Aldrich.

Epoxidation of soybean oil (ESO)

Epoxidation of soybean oil was adapted from the literature procedure [18]. Soybean oil and formic acid were charged into a three-neck flask equipped with a reflux condenser and a mechanical stirring under a nitrogen gas atmosphere. The addition of H_2O_2 starts after 10 h of stirring at 50 °C under a nitrogen gas. The molar ratio of the carbon double bond of soybean oil to H_2O_2 was used as 1:1,7. To prevent fast heating, hydrogen peroxide is introduced gradually/dropwise to the reaction mixture. The reaction was stirred for 7 h at 50 °C, and then, the mixture is cooled to room temperature. To eliminate residual acid, the mixture was diluted and then, washed three times with a 5 wt% $NaHCO_3$. The organic layer was dried with anhydrous sodium sulfate. The product was obtained with an 85% yield. The epoxy content was determined by ASTM D1652-97. The reaction pathway is shown in Scheme 1.

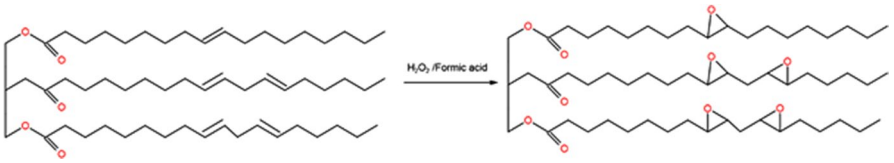

Scheme 1 The epoxidation of soybean oil

Epoxidation of cardanol (ECARD)

Epoxidation of cardanol was adapted from the literature procedure [19]. Cardanol and ZnO_2 in a three-neck round flask were equipped with a reflux condenser and a mechanical stirring under a nitrogen gas atmosphere. The mixture was heated at 90 °C. Epichlorohydrin was added dropwise, to prevent a sudden temperature rise. The mixture was further stirred for 3 h. Then, an aqueous NaOH solution (19.3 g NaOH/100 mL water) was added by a dropping funnel. The reaction temperature was increased to 100 °C and stirred for 2 h. After this period, the product was separated, to remove unreacted impurities and dried. The product obtained in 77% yield. The epoxy content was determined by ASTM D1652-97. The reaction pathway is shown in Scheme 2.

Preparation of sol–gel precursor

The solution was prepared by mixing 2.799 g of TEOS (0.0134 mol), 1.579 g of ethanol (0.034 mol), and 1 g of distilled water (0.056 mol) [20]. The mixture was stirred until a homogenous solution was obtained, and then, the calculated amount of *p*-TSA was added. To create a silane sol, the mixture was stirred continuously for 24 h at room temperature. Finally, GPTMS was added to the sol–gel solution with 5% of the total weight.

Preparation of film and coatings

The coating formulations were prepared by mixing the calculated amount of ECARD, TETA, DGEBA, ESO, sol–gel precursor, and EPOSS. The composition

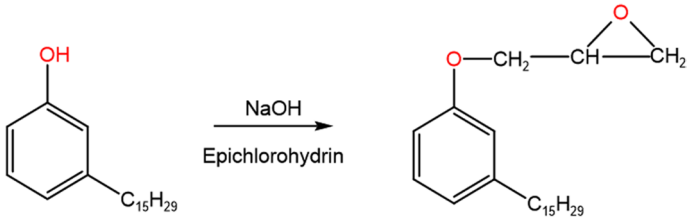

Scheme 2 The epoxidation of cardanol

Table 1 The composition of epoxy coatings

Samples	ECARD (g)	DGEBA (g)	TETA (g)	ESO (g)	SOL–GEL (%)	EPOSS (%)
ECARD-DGEBA	5	5	1.52	–	–	–
ECARD-DGEBA-0.0025P	5	5	1.52	–	2	0.0025
ECARD-DGEBA-0.005P	5	5	1.52	–	2	0.005
ECARD-DGEBA-0.01P	5	5	1.52	–	2	0.01
ECARD-DGEBA-ESO-0.0025P	5	3	1.43	2	2	0.0025

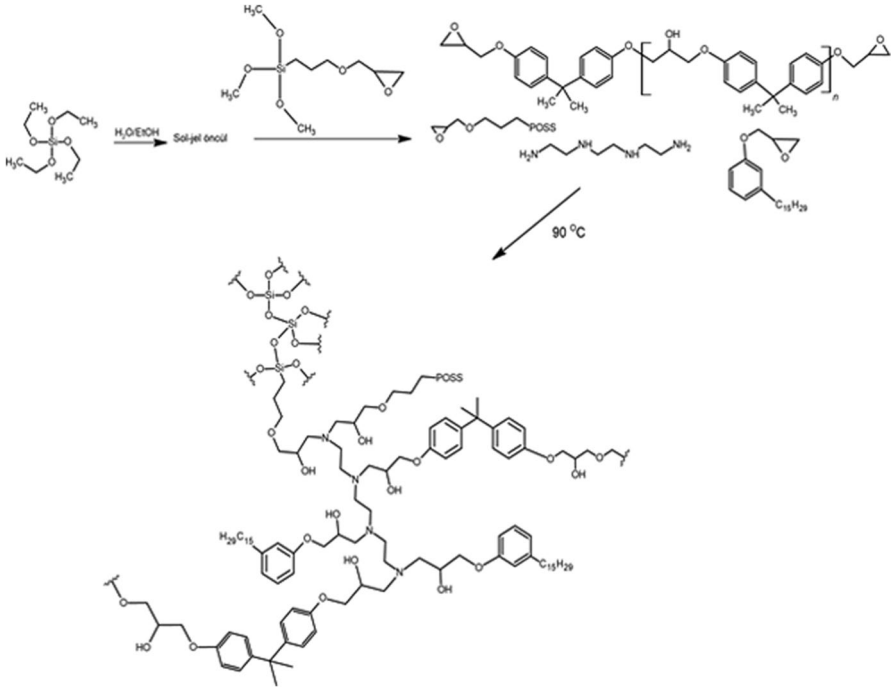

Scheme 3 Preparation pathway of organic–inorganic network

of the samples is shown in Table 1. The prepared liquid formulations were poured into a TEFLON mold, and the temperature gradually increased from 60 °C to the cure temperature of each sample. In addition, the liquid formulations were applied to aluminum sheets. (Scheme 3).

Characterizations

The structural analysis of epoxidized vegetable oils (cardanol and soybean oil) was performed by FTIR (JASCO FT/IR-4200 JASCO Corp) and ^{1}H-NMR (Mercury-VX 400 MHz Spectrometer) spectroscopies. Thermogravimetric analysis (TGA) of the coating materials was performed by the thermogravimetric analyzer (Discovery TGA 55, TA Instruments). Morphological analysis of the films was performed on Philips XL30 ESEM-FEG/EDAX. DSC measurements were performed using Pyris Diamond DSC. The mechanical properties of the films were determined using Zwick Z010 Universal Tensile Tester with a crosshead speed of 10 mm/min. The contact angle measurement of the cured coatings was measured with Kruss Easy Drop DSA-2. AFM images were obtained using an Ambios-Quesant Q-Scope Universal SPM (Scanning Probe Microscope) with AFM attachment, at tapping mode in air atmosphere and at room temperature). The properties of coatings were tested by cross-cut tape adhesion (ASTM D-3359) and pendulum hardness (ISO 1520). The anti-corrosive properties of the coatings were investigated according to ASTM B 117. The dry coating thickness was measured using a PosiTest DFT coating thickness gauge.

Results and discussions

Characterization of ESO and ECARD

Epoxy modification of SO confirmed by FTIR and ^{1}H-NMR spectroscopies. The FTIR spectra of SO and ESO are shown in Fig. S1. The characteristic peaks at 2925 and 2860 cm^{-1} are the asymmetric and symmetric C–H stretching belonging to methylene groups of triglycerides. The peaks at 721, 1648, and 3008 cm^{-1} related to stretching vibrations of double bonds (*cis* CH=CH, C=C, and=C–H) of SO, respectively. After the epoxidation reaction of SO, the disappearance of these peaks shows the success of the epoxidation reaction. The new peaks observed at 775, 852, and 1045 cm^{-1} correspond to the C–O–C stretching of the oxirane ring. The peak of about 1100 cm^{-1} is related to the C–O stretching of the ether group for both spectra [18].

The NMR spectrum of ESO is shown in Fig. S2. The signal at 0.8 ppm corresponds to the methyl protons of the fatty acid chains. The peak at 2.2 ppm is assigned to protons α of the carbonyl groups. CH_2 protons of the glycerol backbone were observed in the range of 4.0–4.2 ppm. Also, the peak at 5.2 ppm corresponds to CH protons of the glycerol unit. The signals in the range of 2.8–3.2 ppm confirmed the existence of epoxy groups. The peaks at 3.1 and 2.9 ppm are due to CH_2 and CH protons of the oxirane ring, respectively [21, 22].

The FTIR spectra of cardanol and epoxy-functionalized cardanol are shown in Fig. S3. As can be seen clearly, the characteristic peaks of epoxy groups were observed at 855, 1045 (asymmetric stretching C–O of the epoxy ring), and 759 cm^{-1} (C–H bending vibration of epoxide ring). In addition, the absence of the olefinic

(CH=CH) double bond peak at 3008 cm^{-1} in the spectrum of ECARD confirmed that the epoxy groups were successfully covalently attached to cardanol.

^{1}H-NMR spectra of cardanol and ECARD are shown in Fig S4. The peak at 7.1 ppm is assigned to aromatic protons of cardanol. The signals in the range of 5.3–5.4 ppm correspond to side chain unsaturation CH=CH of cardanol. CH_2 protons of the side chain of cardanol (–CH_2CH=CHCH_2–) were assigned at 2.04 ppm. The aliphatic protons of side chains were observed in the range of 1, 4–1.2 ppm [23]. The new peaks corresponding to the protons of the epoxy unit appear in the region of 2.2–2.6 ppm.

Structural characterization of the bio-based nanocomposites

FTIR spectra of bio-based nanocomposites with various DEGBA, ECARD, and ESO contents are shown in Fig. S5. The broadband in the 3600–3200 cm^{-1} region corresponds to the secondary hydroxyl groups of the ring-opening reaction of oxiranes. The peak at 2900–2800 cm^{-1} is due to C–H stretching. The signals at 1100 and 1245 cm^{-1} are ascribed to the C–O asymmetric stretching. The peak at 855 and 1045 cm^{-1} disappeared due to the opening of epoxy groups by the epoxy-amine curing reaction. The new peak in the region of 1037 cm^{-1} belongs to the C–N stretching peak. The increase in the intensity of 825 and 1245 cm^{-1} peaks is attributed to the addition of POSS and sol–gel, which are due to the overlapping Si–O–Si stretching with C–O str.

Curing reaction mechanism

In this study, the epoxy groups are easily opened in the presence of a TETA hardener without the use of any catalyst via the SN_2 reaction mechanism. TETA is widely used as an oxirane-curing agent for preparing epoxy coatings. Organic salt catalysts (e.g., Zinc II) are often used for the preparation of cross-linked epoxy thermoset through epoxy-amine reaction [24]. However, most of them are toxic and cause corrosion; therefore, it is preferred to achieve fast and effective curing without the need for a catalyst [25]. The cure profiles of the liquid formulations were investigated by DSC. The curing of epoxy resin with TETA and the curing of nanocomposite formulations were studied and compared. Figure 1a shows the exothermic curing profiles of the DGEBA, ECARD, and ESO resins individually with the TETA curing agent. The peak maximum temperature (T_{max}) and total heat of the reaction (ΔH) can be seen in Fig. 1a. DGEBA showed the lowest temperature peak with respect to the ECARD and ESO systems. This indicates the reactivity of epoxides is DGEBA > ECARD > ESO. The decreasing trend in the enthalpy of the reaction was also observed as $\Delta H_{ESO} < \Delta H_{ECARD} < \Delta H_{DGEBA,}$ suggesting less crosslinking occurred by using ESO. This was probably due to the higher chain length and lower epoxy content of the ESO [25]. Generally, internal epoxies on the long aliphatic chains show less reactivity than terminal epoxies. It is reported that curing processes of ESO take place at higher temperature and longer times with respect to bisphenol A epoxy resin [26, 27]. In Fig. 1b, the well-defined single exothermic

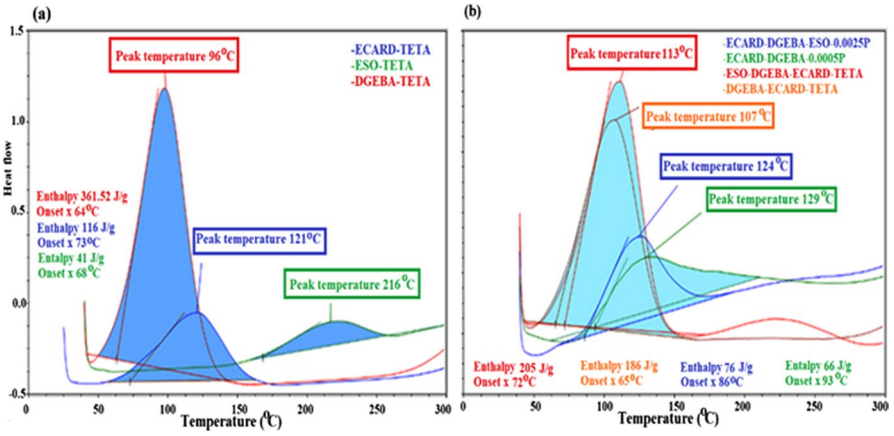

Fig. 1 The curing profiles liquid epoxy formulations **a** DGEBA, ECARD, and ESO, **b** ECARD-DGEBA, ECARD-DGEBA-ESO, ECARD-DGEBA-0.0025P, and ECARD-DGEBA-ESO-0.0025P

peak was observed for DGEBA, ECARD, and TETA mixture with peak temperature at 108 °C, indicating that the DGEBA and ECARD are compatible with each other. However, the analysis indicated that the addition of ESO into the epoxy mixture raises the peak temperature (111 °C) of the curing process. In addition, a slight second peak at 220 °C can be seen due to the immiscibility of ESO. Steric hindrance probably caused this observation resulting in retardation of the curing process. In the case of nanocomposites, the cure temperature of the ECARD-DGEBA-0.0025P, and ECARD-DGEBA-ESO-0.0025P shifted to a higher temperature due to the presence of EPOSS and sol–gel. The bulky POSS can cause sterically hinder the reaction of the epoxy-amine groups. However, the DSC thermograms of both nanocomposites are very smooth and have only a single curing peak [28]. This demonstrates that the compatibility between the three resin systems was attained by using EPOSS and GPTMS containing sol–gel.

Glass transition temperatures of nanocomposite films

The glass transition temperature (T_g) of the nanocomposite films was measured by DSC. The DSC curves are shown in Fig. S6. T_g values are also given in Table 2. The T_g of ECARD-DGEBA was found as 45 °C. The epoxidized vegetable oil-based films typically have a lower T_g [29]. The T_g value for ECARD-DGEBA-0.01P slightly increased from 43 to 45 °C with the addition of EPOSS and sol–gel. However, the T_g values showed a significant increase with the increase in EPOSS content (0.005 and 0.01) to 66 °C and 98 °C, respectively. The increase in T_g might be related to the mobility of the polymer chain. Cross-linked network structure may occur by the further condensation possibilities of silanol groups on POSS. Hence, the chain mobility restricts and raises the T_g of the films [30]. ECARD-DGEBA-ESO-0.0025P had a slightly higher T_g than ECARD-DGEBA-0.0025P, due to the epoxy groups on ESO structure incorporated to network formation [31].

Table 2 TGA and DSC results of the nanocomposites

Sample no	$T_{5\%}$ (°C)	$T_{50\%}$ (°C)	Char (%)	T_g (°C)
ECARD-DGEBA	250	384	0	43
ECARD-DGEBA-0.0025P	308	392	2.82	45
ECARD-DGEBA-0.005P	312	388	2.41	66
ECARD-DGEBA-0.01P	315	388	3.66	98
ECARD-DGEBA-ESO-0.0025P	281	392	3.17	60

Epoxidized-POSS as a coupling agent probably provided the increase in crosslink density between the organic and the inorganic parts. The T_g of the films increased because of the restriction of chain mobility [32].

Thermal stability

Thermal analysis of the nanocomposite films was evaluated by thermogravimetric analysis. The curves of the films and weight loss temperatures are shown in Fig. 2 and Table 2, respectively. 5 wt% weight loss was seen between 250 and 315 °C. As can be seen, all formulations exhibited a two-stage degradation profile. The first weight loss was observed from 300 to 450 °C because of the thermal degradation of the polymer backbone. The second weight loss is due to the presence of sol–gel and EPOSS. When the EPOSS content was increased, the first and second thermal degradation temperatures of the films shifted toward a slightly higher temperature. EPOSS has a rigid nanocage framework. This structure effectively enhances the

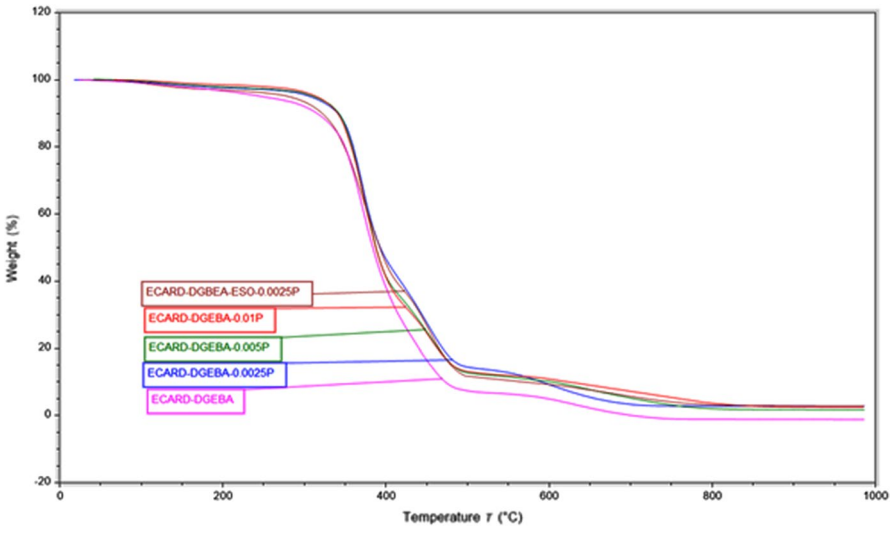

Fig. 2 TGA curves of the nanocomposite films

thermal stability of the films as compared to the sample ECARD-DGEBA due to the stable Si–O–Si linkages [33]. In addition, the char yield of the samples containing sol–gel and EPOSS tends to increase compared to ECARD-DGEBA. Above 600 °C, the ECARD-DGEBA-0.05P showed the highest thermal stability and the highest char yield.

Mechanical properties of films

Mechanical properties of the nanocomposites were characterized by Young's modulus, elongation at break, and tensile strength. The results are shown in Table 3. The hybrid composites have a higher elongation at break values than ECARD-DGEBA film. The flexible secondary hydroxyl functionalities that occurred through the ring-opening reaction of EPOSS with amine groups provide an increase in elongation [34]. In addition, the Young's modulus and tensile strength values of the hybrid composites were significantly improved with the addition of EPOSS and sol–gel. Consequently, a serious improvement in the mechanical properties of the nanocomposites indicates strong compatibility between sol–gel, EPOSS, and matrix [35]. For ECARD-DGEBA-ESO-0.0025P, modulus, and tensile strength decreased as expected. On the other, the elongation at break reached 81% because of the long side alkyl chains of ESO [36].

Morphological and surface characterizations

The dispersion of EPOSS and epoxy-end capped silane sol–gel in the epoxy network was investigated via SEM technique. The SEM images of the fractured surface at 100.000X magnification are shown in Fig. 3. As can be seen in the images, particles were well dispersed in the polymer matrix without agglomeration. The modification of hydrophobic POSS particles with silanol groups helps to achieve good dispersion [37].

The elemental composition of ECARD-DGEBA-0.0025P was also examined using EDS analysis (Fig. 4). Three peaks were observed corresponding to C, O, and Si in the EDS spectra of ECARD-DGEBA-0.0025P. The atoms C, O, and Si were assigned as 77%, 16%, and 7%, respectively.

Table 3 Tensile stress–strain test results of the nanocomposite films

Samples	Young's modulus (MPa)	Tensile strength (MPa)	Elongation at break (%)
ECARD-DGEBA	5	15	20
ECARD-DGEBA-0.0025P	66	28	39
ECARD-DGEBA-0.005P	69	30	35
ECARD-DGEBA-0.01P	88	32	27
ECARD-DGEBA-ESO-0.0025P	1	3	81

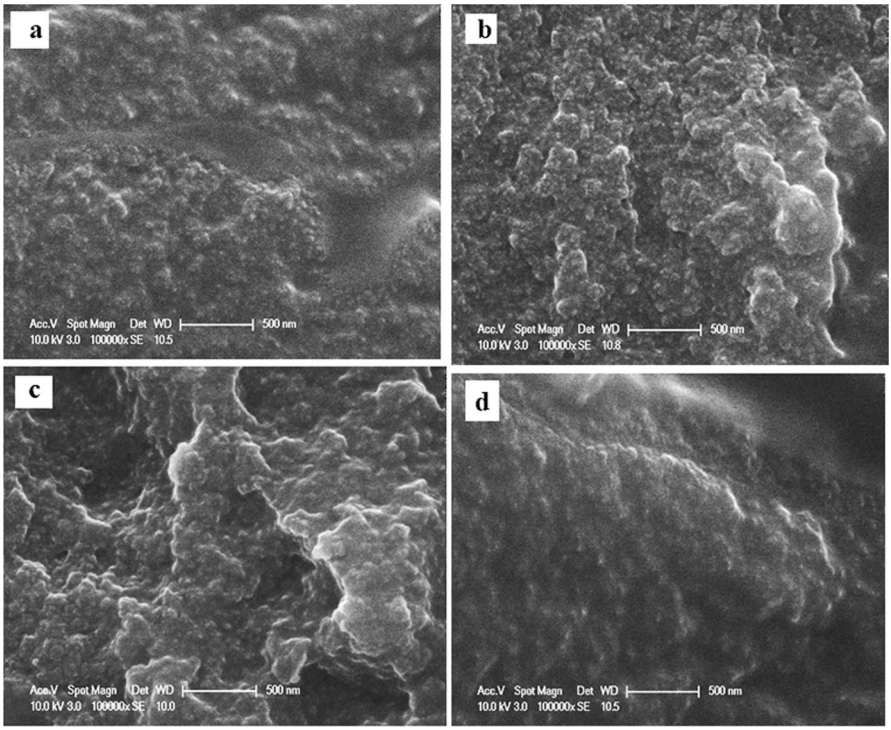

Fig. 3 SEM images of **a** ECARD-DGEBA-0.0025P, **b** ECARD-DGEBA-0.005P **c** ECARD-DGEBA-0.01P **d** ECARD-DGEBA-ESO-0.0025P at 100.000 × magnifications

Two- and three-dimensional topographic AFM images of nanocomposites are presented in Fig. 5 at different magnifications. The surface of the films with various EPOSS compositions is rough with numerous ‘’peaks” and ‘’valleys”. In addition, the oriented microstructure similar to the cage structure of POSS was observed. Table 4 summarizes the roughness measured by AFM for ECARD-DGEBA-0.0025P, ECARD-DGEBA-0.005P, and ECARD-DGEBA-ESO-0.0025P films. As can be seen that the surface roughness increases with EPOSS concentration. The surface roughness (RMS) of the films was found as 65 nm (432 nm in height) and 143 nm (727 nm in height), respectively, for ECARD-DGEBA-0.0025P (Fig. 5a) and ECARD-DGEBA-0.005P (Fig. 5b). From these results, it was concluded that, as the concentration of the EPOSS increased, surface roughness increased due to formation of agglomerated POSS particles. Moreover, surface roughness was affected by the structure of epoxy resin as well as the dispersion of nanoparticles. The surface roughness was found at 71 nm for the ECARD-DGEBA-ESO-0.0025P film (Fig. 5c). The surface roughness of the ECARD-DGEBA-ESO-0.0025P film was decreased due to the lubrication effect of vegetable oils compare with ECARD-DGEBA-0.005 having same EPOSS content [37].

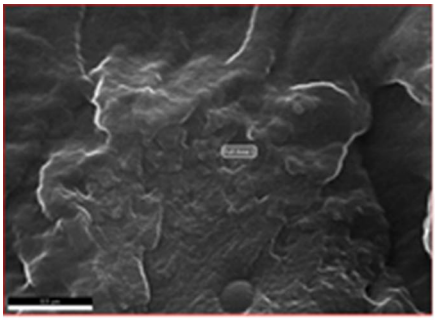

Smart Quant Results

Element	Weight %	Atomic %	Error %
New Project | New Sample | IzelKimya1poss15 | Full Area 1			
C K	77.09	83.85	8.78
O K	15.64	12.77	27.28
Si K	7.28	3.39	5.77

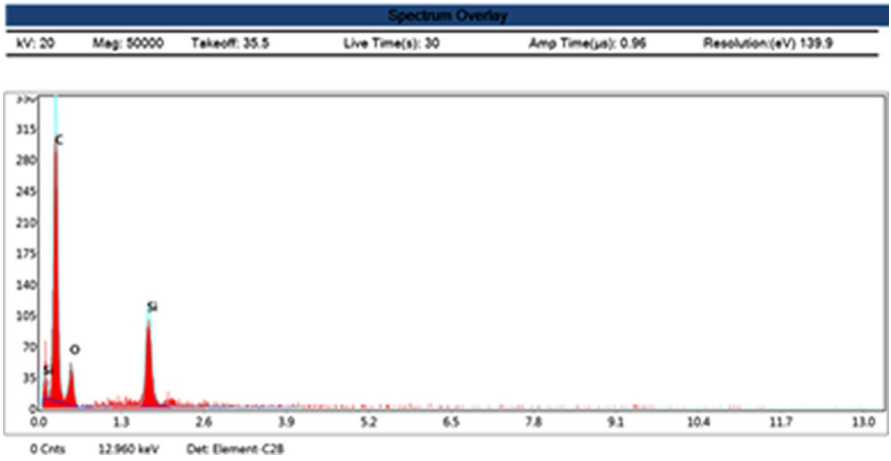

Fig. 4 EDS spectrum of ECARD-DGEBA-0.0025P

Coating properties

The properties of the coatings were also investigated. The contact angle, salt spray, crosscut adhesion, pendulum hardness test results, and film thickness are presented in Table 5.

The wettability of the nanocomposite coatings was evaluated by the water contact angle test. The water contact angle images of the coatings are shown in Fig. 6. As can be seen, the contact angle of ECARD-DGEBA was 60°. The addition of EPOSS to the formulation leads to an increase in surface hydrophobicity by reducing surface energy [38]. Compared to the base formulation, the water contact angle of all the nanocomposite coatings increased. The contact angles increased due to the reaction of the active groups of silanes of TEOS and EPOSS through a sol–gel reaction [17]. Moreover, at the same amount of EPOSS and sol–gel content ESO containing coating showed a lower contact angle of 67°. The

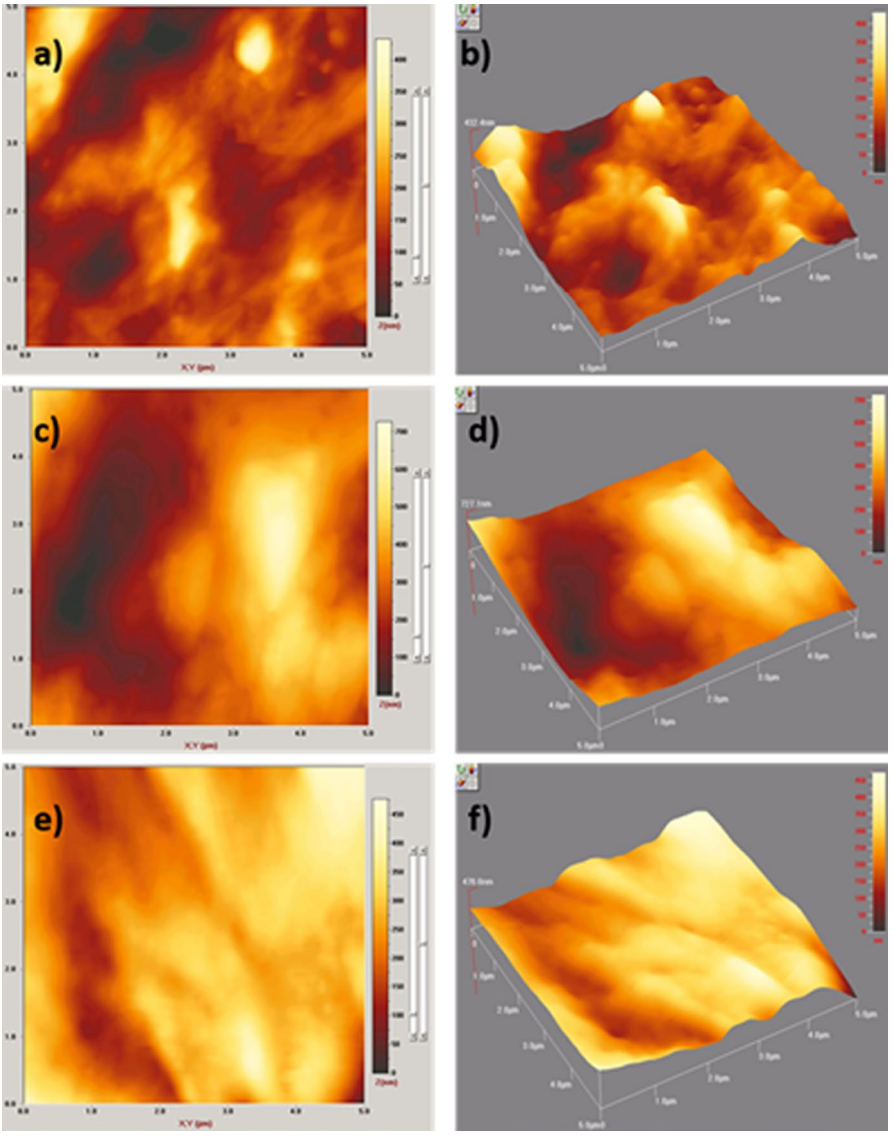

Fig. 5 AFM images of the coatings

Table 4 Surface roughness from AFM results

Samples	Average roughness (nm)	Peak valley roughness (nm)	RMS (nm)
ECARD-DGEBA-0.0025P	49	432	65
ECARD-DGEBA-0.01P	11	727	143
ECARD-DGEBA-ESO-0.0025P	57	476	71

Table 5 The coating performance of nanocomposites

Samples	Contact angle (°)	Crosscut adhesion	Pendulum hardness (Persoz-sec)	Film thickness (μm)
ECARD-DGEBA	60	0	85	42
ECARD-DGEBA-0.0025P	74	0	120	40
ECARD-DGEBA-0.005P	75	0	137	50
ECARD-DGEBA-0.01P	78	0	176	46
ECARD-DGEBA-ESO-0.0025P	67	0	53	46

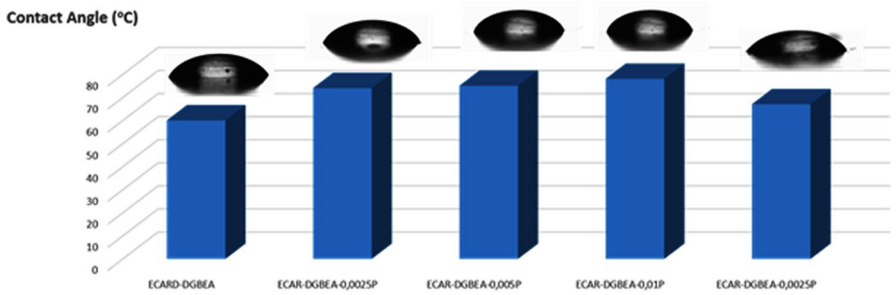

Fig. 6 Contact angles of the coatings

reduction in the contact angle value may be related to the increase in hydroxyl groups after the epoxy ring opening of ESO.

The anti-corrosion properties of the coating were investigated by a salt spray test. The coatings were held in a salt spray chamber at aggressive salt conditions by using seawater for 350 h. The photographs of the coating are shown in Fig. 7. All coatings showed strong salt spray resistance. The long alkyl groups of cardanol provided a strong barrier effect. Additionally, the hydrophobicity of the coating surfaces provides a barrier at the interface and prevents corrosive groups from diffusing through the coating's surface [39].

The crosscut adhesion test was applied for all cured coatings. The results demonstrated effective interaction between the coating formulations and aluminum panels. The excellent adhesion could be attributed to the high crosslink density [40].

The hardness properties of the coatings were evaluated by pendulum hardness. The results of the pendulum hardness test are given in Table 5. The flexibility of the film affects damping time. The ability of the film to absorb pendulum energy increases with its flexibility and therefore pendulum time decreases [41]. As can be seen, the pendulum hardness increased with the increased amount of EPOSS and sol–gel contents. The highest pendulum hardness (176 s) was observed for the ECARD-DGEBA-0.01P film. However, ECARD-DGEBA-ESO-0.0025P showed a value of 53 s. This could be explained by the presence of flexible long aliphatic chains of ESO.

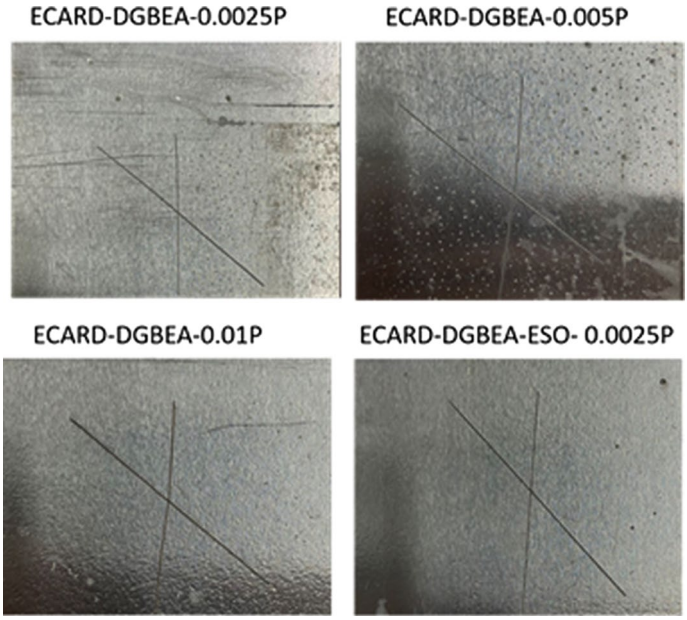

Fig. 7 Salt spray images of coatings

Conclusion

In recent years, developing novel polymeric materials has been significantly assisted by bio-based derivatives made from sustainable resources like cardanol and soybean oil. In this study, we created a straight way to prepare bio-based epoxy coatings derivable from natural resources without the use of any catalyst. The coatings exhibited acceptable thermal and mechanical stability according to the thermal and mechanical results. The prepared coatings are stable up to 300 °C. Furthermore, the samples exhibited satisfactory mechanical properties. With the incorporation of only 0.01 wt % POSS, Young's modulus was increased more than tenfold. At the same time, the bio-based coatings exhibited excellent anti-corrosive resistance even though no anti-corrosive additives were used.

Supplementary Information The online version contains supplementary material available at https://doi.org/10.1007/s00289-023-05037-4.

Acknowledgements The financial support for this work by İZEL KİMYA and The Scientific and Technological Research Council of Turkey (TUBITAK)-Technology and Innovation Funding Programs Directorate (TEYDEB) under the project 3191518 is gratefully acknowledged. We would like to thank Levent BABAYİĞİT for conducting analyses.

Author contributions SE contributed to investigation, and writing—original draft. BO contributed to investigation, and writing—original draft. CD contributed to supervision, and writing—review & editing. NKA contributed to supervision, and writing—review & editing.

Declarations

Conflict of interest The authors declare that no conflict of interest exists related to this publication.

References

1. Luo X, Gao F, Chen F, Cheng Q, Zhao J, Wei X, Shen L (2020) Organic–inorganic hybrid coating materials derived from renewable soybean oil and amino silanes. RSC Adv 10(27):15881–15887
2. Di Mauro C, Malburet S, Genua A, Graillot A, Mija A (2020) Sustainable series of new epoxidized vegetable oil-based thermosets with chemical recycling properties. Biomacromolecules 21(9):3923–3935
3. Liang B, Chen J, Guo X, Yang Z, Yuan T (2021) Bio-based organic-inorganic hybrid UV-curable hydrophobic coating prepared from epoxidized vegetable oils. Ind Crops Prod 163:113331
4. Bobade SK, Paluvai NR, Mohanty S, Nayak SK (2016) Bio-based thermosetting resins for future generation: a review. Polym-Plast Technol Eng 55(17):1863–1896
5. Puchot L (2016) Cardanol: a bio-based building block for new sustainable and functional materials. PhD Thesis. Cergy-Pontoise
6. Caillol S (2018) Cardanol: a promising building block for biobased polymers and additives. Curr Opin Gr Sustain Chem 14:26–32
7. vom Saal FS, Myers JP (2008) Bisphenol A and risk of metabolic disorders. JAMA 300(11):1353–1355
8. Baker NF (1955) Epoxy resin compositions, US Patent 824 302
9. Zhao S, Abu-Omar MM (2015) Biobased epoxy nanocomposites derived from lignin-based monomers. Biomacromolecules 16(7):2025–2031
10. Pascault JP, Williams RJ (2009) Epoxy polymers: new materials and innovations. John Wiley & Sons, New York
11. Du Y, Shi G, Wang J, Wang Y, Wang X, Wang L, Ren S (2022) Influences of POSS-E-GO content on mechanical properties of bio-based epoxy/DOPO-POSS nanocomposites. J Wuhan Univ Technol-Mater Sci Ed 37(4):765–772
12. Aziz T, Fan H, Haq F, Khan FU, Numan A, Iqbal M, Wazir N (2020) Adhesive properties of poly (methyl silsesquioxanes)/bio-based epoxy nanocomposites. Iran Polym J 29(10):911–918
13. Mohamed MG, Mansoure TH, Takashi Y, Samy MM, Chen T, Kuo SW (2021) Ultrastable porous organic/inorganic polymers based on polyhedral oligomeric silsesquioxane (POSS) hybrids exhibiting high performance for thermal property and energy storage. Microporous Mesoporous Mater 328:111505
14. Zhang W, Li X, Yang R (2011) Pyrolysis and fire behaviour of epoxy resin composites based on a phosphorus-containing polyhedral oligomeric silsesquioxane (DOPO-POSS). Polym Degrad Stab 96(10):1821–1832
15. Florea NM, Lungu A, Badica P, Craciun L, Enculescu M, Ghita DG, Iovu H (2015) Novel nanocomposites based on epoxy resin/epoxy-functionalized polydimethylsiloxane reinforced with POSS. Compos B Eng 75:226–234
16. Olson E, Liu F, Blisko J, Li Y, Tsyrenova A, Mort R, Jiang S (2021) Self-assembly in biobased nanocomposites for multifunctionality and improved performance. Nanoscale Adv 3(15):4321–4348
17. Chen S, Guo L, Du D, Rui J, Qiu T, Ye J, Li X (2016) Waterborne POSS-silane-urethane hybrid polymer and the fluorinated films. Polymer 103:27–35
18. Diez-Pascual AM, Diez-Vicente AL (2014) Epoxidized soybean oil/ZnO biocomposites for soft tissue applications: preparation and characterization. ACS Appl Mater Interfaces 6(19):17277–17288
19. Suresh KI, Kishanprasad VS (2005) Synthesis, structure, and properties of novel polyols from cardanol and developed polyurethanes. Ind Eng Chem Res 44(13):4504–4512
20. Oktay B, Kayaman-Apohan N (2013) Maleimide containing UV-cured hybrid coatings. Adv Polym Technol. https://doi.org/10.1002/adv.21341
21. Khot SN, Lascala JJ, Can E, Morye SS, Williams GI, Palmese GR, Wool RP (2001) Development and application of triglyceride-based polymers and composites. J Appl Polym Sci 82(3):703–723
22. Zhou J, Wang W, Villarroya S, Thurecht KJ, Howdle SM (2008) Epoxy functionalised poly (ε-caprolactone): synthesis and application. Chem Commun 44:5806–5808

23. Rekha N, Asha SK (2008) Synthesis and FTIR spectroscopic investigation of the UV curing kinetics of telechelic urethane methacrylate crosslinkers based on the renewable resource—cardanol. J Appl Polym Sci 109(5):2781–2790
24. Hao C, Liu T, Zhang S, Liu W, Shan Y, Zhang J (2020) Triethanolamine-mediated covalent adaptable epoxy network: excellent mechanical properties, fast repairing, and easy recycling. Macromolecules 53(8):3110–3118
25. Hernandez NLP, Bonon AJ, Bahú JO, Barbosa MIR, Maciel MRW, Maciel Filho R (2017) Epoxy monomers obtained from castor oil using a toxicity-free catalytic system. J Mol Catal A: Chem 426:550–556
26. Tang Q, Chen Y, Gao H, Li Q, Xi Z, Zhao L, Peng C, Li L (2018) Bio-based epoxy resin from epoxidized soybean oil. In: Kasai M (ed) Soybean-biomass, yield and productivity. IntechOpen, London. https://doi.org/10.5772/intechopen.81544
27. Zhao CH, Wan SJ, Wang L, Liu XD, Endo T (2014) Carbonyldiimidazole-accelerated efficient cure of epoxidized soybean oil with dicyandiamide. J Polym Sci, Part A: Polym Chem 52(3):375–382
28. Gao J, Kong D, Li S (2008) Preparation of BPA epoxy resin/POSS nanocomposites and nonisothermal co-curing kinetics with MeTHPA. Int J Polym Mater 57(10):940–956
29. Oktay B, Türkcan JH, Özdemir OK, Kayaman-Apohan N (2023) Vegetable oil-based epoxy coating materials for self-healing and anticorrosive applications. Macromol Res. https://doi.org/10.1007/s13233-023-00190-1
30. Balani K, Verma V, Agarwal A, Narayan R (2014) Physical, thermal and mechanical properties of polymers. In: Biosurfaces. John Wiley & Sons, Hoboken
31. Kinaci E, Can E, Scala JJL, Palmese GR (2020) Influence of epoxidized cardanol functionality and reactivity on network formation and properties. Polymers 12(9):1956
32. Baştürk E, Oktay B, Kahraman MV (2015) Dual-crosslinked thiol-ene/sol gel hybrid electrospun nanowires: preparation and characterization. J Polym Res 22:1–7
33. Dou Q, Abdul Karim A, Loh XJ (2016) Modification of thermal and mechanical properties of PEG-PPG-PEG copolymer (F127) with MA-POSS. Polymers 8(9):341
34. Hu Y, Shang Q, Wang C, Feng G, Liu C, Xu F, Zhou Y (2018) Renewable epoxidized cardanol-based acrylate as a reactive diluent for UV-curable resins. Polym Adv Technol 29(6):1852–1860
35. Zhao Y, Schiraldi DA (2005) Thermal and mechanical properties of polyhedral oligomeric silsesquioxane (POSS)/polycarbonate composites. Polymer 46(25):11640–11647
36. Tathe DS, Jagtap RN (2015) Biobased reactive diluent for UV-curable urethane acrylate oligomers for wood coating. J Coat Technol Res 12(1):187–196
37. Manh Vu C, Bach QV, Duong LX, Thai NV, Thao VD, Duc PT, Van Nguyen T (2020) Silane coupling agent with amine group grafted nano/micro-glass fiber as novel toughener for epoxy resin: fabrication and mechanical properties. Compos Interfaces 27(12):1085–1100
38. Shreeshail ML, Desai AC, Siddhalingeshwar IG, Kodancha KG (2021) A study on influence of vegetable oils in milling operation and it's role as lubricant. Mater Today: Proc 46:2699–2713
39. Ou J, Hu W, Xue M, Wang F, Li W (2013) Superhydrophobic surfaces on light alloy substrates fabricated by a versatile process and their corrosion protection. ACS Appl Mater Interfaces 5(8):3101–3107
40. Kathalewar M, Sabnis A (2014) Epoxy resin from cardanol as partial replacement of bisphenol-A-based epoxy for coating application. J Coat Technol Res 11(4):601–618
41. Denis M, Totee C, Le Borgne D, Caillol S, Negrell C (2022) Cardanol-modified alkyd resins: novel route to make greener alkyd coatings. Prog Org Coat 172:107087

Authors and Affiliations

Semiha Eral[1,2] · Burcu Oktay[2] · Cemil Dizman[1] · Nilhan Kayaman Apohan[2]

✉ Cemil Dizman
cemil.dizman@izelkimya.com.tr

✉ Nilhan Kayaman Apohan
napohan@marmara.edu.tr

[1] İzel Kimya Research and Development Center, Dilovası, Kocaeli, Turkey

[2] Department of Chemistry, Marmara University, 34722 Kadıköy, Istanbul, Turkey